VOID CHARACTERIZATION AND MEMBRANE SELECTION IN THE VACUUM ASSISTED PROCESS

A. George[1*], K. Drechsler[2]

[1]*Swerea SICOMP AB, PO Box 271, SE-94126, Piteå, Sweden*
[2]*Institute of Aircraft Design, Stuttgart University, Pfaffenwaldring 13, DE-75069 Stuttgart, Germany*
**andy.george@swerea.se*

Keywords: VAP, voids, porosity, resin infusion.

Abstract
The Vacuum Assisted Process (VAP) can achieve better laminate quality than other infusion processes. This study aims to develop void characterization tools, to characterize the resultant void content in VAP, and to evaluate various membranes with respect to laminate quality. Infusions were made with each membrane and either single- or double-sided distribution media coverage. Each laminate's thickness gradient was measured, as well as the void content by three methods for comparison. The voids' position and size were characterized. The ultrasound attenuation and the shear strength were correlated to the local void content.

1 Introduction
Resin infusion (RI) is increasingly being used by industry to manufacture composite parts due to its low cost compared to autoclave manufacturing. A patented [1] variant for high-quality and thick parts is the Vacuum Assisted Process (VAP). A semi-permeable membrane separates the vacuum outlet from the surface of the part. This creates a full vacuum gradient and continued degassing across the part surface. Air no longer has to pass through the entire preform before being evacuated. This results in fewer voids and reduced thickness gradients, thus higher mechanical properties and repeatability [2]. For a membrane to function correctly, it must not be saturated by the resin for the duration of infusion to cure. A larger pore size allows more degassing, but would also allow for quicker membrane saturation. Membranes are usually either polytetraflouroethylene (PTFE) or polyurethane (PUR). The aim of this study is three-fold: to develop void characterization tools, to characterize the resultant void content in VAP, and to evaluate various membranes in respect to laminate quality.

The void content, v_0, is the volumetric percentage of air in the final part. The simplest method to measure v_0 is volume comparison. An approximate volume of all solids and voids is calculated by multiplying the measured thickness, h, by the laminate's length and width. The actual volume of all solids is then calculated from the measured weights of the dry preforms and cured laminates, the difference being the resin weight, and the densities of each component. The difference between these two volumes is the volume of air. A problem with this method is the rounded edges and the irregular h (peel-ply pitting), which depart from the assumed ideal geometry. This method gives an easily obtained bulk measurement of v_0 without the need for many tests of the same sample. Optical measurement of voids has been

the most popular of v_0 measurement methods [3,4]. Images are examined for the darkest areas signifying voids. A gray-scale threshold must properly delineate the void areas and can add some operator-subjectivity to the measurement. This requires fine polishing of each sample, and treatment of each image to ensure that non-void features are not included in the areal count. This method actually measures the void size itself, but is also the least straight-forward. Digestion methods involve dissolving the resin from a laminate sample. The sample's weight before digestion and the weight of the remaining fibers are compared with the samples pre-digestion density. This method entails little subjectivity, but the void size/location cannot be characterized. This also requires the use of hazardous chemicals and density testing can be inaccurate with porous samples. Ultrasonic c-scan inspection is a non-destructive technique (NDT) to detect defects [4,5]. This requires extensive calibration; any difference in material or thickness implies changes in density which must be accounted for before comparing results.

High variation exists with each of these methods [3]. To predict mechanical failure, the maximum local v_0 must be determined and assumed as the weak link of the part. With proper degassing and sealing, the only air in an epoxy RI infusion comes from entrapment at the flow front. With a constant flow-rate and if the bubbles remained stationary, the laminate would show a homogeneous void distribution. But bubble movement [6,7] and bubble dissolution [8] prevent this ideal scenario. Void prediction models are currently in development [6,9] but require enhancement to accurately predict this. Thus local v_0 measurement remains an important task, and many measurements are required for adequate characterization.

2 Materials and testing methods

The membranes used in this study are listed in Table 1. The membranes "pur1" and "pur2" are the same PUR membrane but with different support fabric materials. The "pur3" membrane is a thicker, un-backed version of the other PUR membranes, with only 10% of their air permeability.

ID	Membrane	Support
ptfe	PTFE	Light Blue PES
pur1	PUR	Light Blue PES
pur2	PUR	White Nylon 6,6
pur3	Double-thick PUR	None

Table 1. Evaluated membranes.

Two infusions were made with each membrane: one infusion with the entire top covered in distribution media (DM) and the second infusion with DM on both the top and bottom. A layer of peel-ply was placed between all layers of DM and the fabric. The reinforcement used was an 8 ply ([0/90/0/90]s), 300 mm x 150 mm stack of a carbon UD weave (272 gsm). The resin used was Huntsman Araldite LY 5052. To better assess the membrane's ability to degas the resin, no resin degassing was performed before the infusion. Vacuum pressure of 50 mbar was applied to a breather cloth above the membrane. The resin was infused at room temperature, with the tool at 40°C. The infused resin amount was controlled by monitoring the weight of the resin pot and allowing enough into the cavity to result in ~40 grams of resin in the laminate. Each infusion took 2 to 3 minutes. The final fiber content (by measurement of h, neglecting v_0) of each infusion ranged from 60.5% to 63.3%.

After infusion, the laminate was left at 40°C for 22 hours for cure, followed by a four hour post-cure at 100°C. A c-scan ultrasound measurement was then made of each laminate's surface using a Sonatest RapidScan2 and 50mm phased array wheel probe. A 10mm strip was then cut from the middle along the 300 mm length. The strip's *h* was measured along the length. It was then sectioned into 10 mm x 20 mm samples, numbered from 1 to 13 based on position (1 by inlet, 13 by opposite end). Measurements of v_0 were made at three locations along the flow path: by the inlet, in the middle, and on the end. Samples 1, 7, and 13 were used in optical void measurements. Samples 2 and 8 were used in solvent digestion void measurements as per ASTM D3171, Method A. The density was measured for all digestion samples using an Accupyc pycnometer. The remainder of the samples was tested for inter-laminar shear strength (ILSS) as per prEN-2563.

These and various other membranes were also used in a similar separate study detailed in [10]. The reinforcement for each of those infusions was a 4-ply carbon biax NCF (540 gsm). A different room-temperature curing epoxy, Hexion MGS RIM 235, was used. Those separate results will be referenced in this study for comparison.

3 Results

3.1 Membrane wetting

The "ptfe" and "pur1" membranes showed insignificant membrane wetting implying good applicability for this 40°C curing epoxy. The "pur2" and "pur3" membranes showed slight membrane wetting; no significant leakage, but some breather fibers stuck to the membrane. This implies that a different support material or the absence of a support material can slightly change the wettability. The PES support on "pur1" may add some resin flow resistance.

Of these 4 membranes, only the PTFE membrane works with epoxy infusions at 120°C. Supplemental VAP infusions were made with Hexcel RTM 6 with each of these membranes. Significant bag wetting and resin loss occurred with any of the PUR membranes. The "pur3" membrane allowed the least resin loss and resulted in a satisfactory part despite the leakage, almost as if it were a large vent with flow resistance. The larger pores of the PUR membranes are suspected to allow resin breakthrough at a sufficiently low viscosity.

3.2 Thickness gradient

Thickness gradients were negligible for all infusions. Figure 1 shows *h* along the length of the infused part for select laminates. Also shown for comparison is the average *h* measurement by a micrometer of the ILSS samples. On the left of Figure 1 are the PTFE infusions, both single DM and double DM. On the right is the same for the "pur1" infusions. No high *h* by the inlet was observed as would be the case without a membrane, for a RI infusion under a vacuum bag. The cause of the 0.1 mm difference between the two membrane types is unknown.

3.3 Void Measurement

Samples for optical v_0 measurement were cast in epoxy plugs and then polished along one long edge. Four images were captured along the polished length, with magnification to barely fit the entire sample *h* in the image. These images were then imported into Image-J. Gray-level thresholding was performed to find the areal percent of dark areas which corresponds to

the v_0. A high degree of light exposure was used for the imaging as this seems to polarize the color levels, thus taking some of the ambiguity out of what threshold level to use.

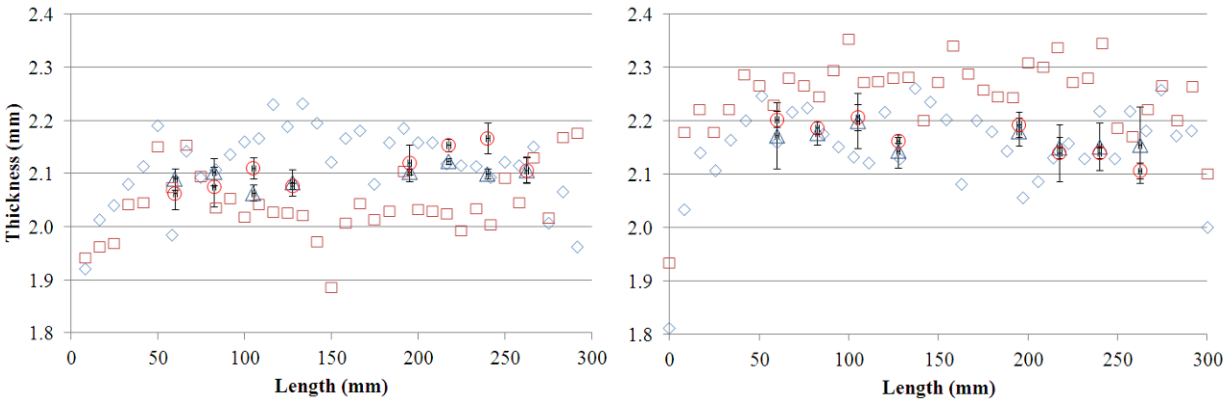

Figure 1. Sample thickness along infusion length: "ptfe" (left) and "pur1" (right); single DM (◊), double DM (□), calipers single DM (Δ), calipers double DM (○).

Some dark areas were painted white in Image-J before measuring v_0 as certain non-void features are dark (binder, stitching threads, cracks from polishing). An example is shown in Figure 2, where one of the original images for the "ptfe" single DM laminate is shown on the left noting various features. The binary image with all image alterations is ready for threshold-application and v_0 measurement. Any area off of the sample was subtracted from the image area before calculating v_0. The measured concentration of voids was split into micro- and macro-voids. Micro-voids are considered to be anything within the fiber tows, while macro-are anything along the edges or in between the tows. The area percent of each is reported as v_{0m} (micro), v_{0M} (macro), and v_{0T} (total). As seen in Figure 2, four of the eight layers have fibers parallel to the polishing surface. These were all painted over as polishing of these layers results in fiber breakage from the small misalignment of the fibers. The v_{0m} for the other layers was measured and then multiplied by 2 to give an estimate of both 0° and 90° layers.

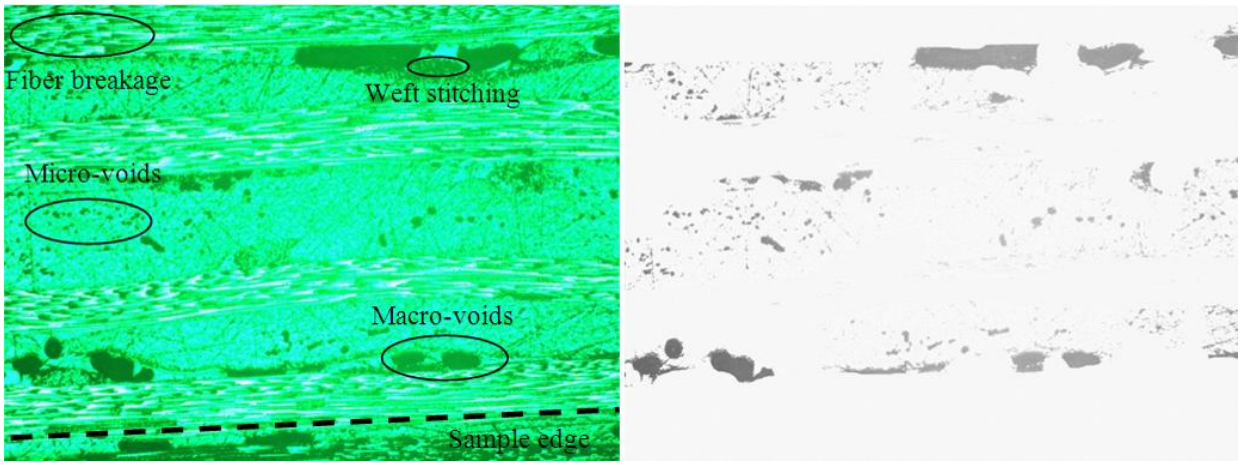

Figure 2. Optical v_0 measurement: original image (left), binary image for v_0 measurement (right).

Figure 3 shows the comparison for v_{0T} as measured by all three methods, as well as the average v_{0m}, v_{0M}, and v_{0T} along with the standard deviation. The laminate labels are preceded by a number denoting how many sides were covered with DM. Note that only select samples were tested by the digestion method for comparison to the other methods. The volume comparison method seems to give fairly comparable results to the other methods, with the

exception of the two highest v_0 laminates: "2-ptfe" and "2-pur1." The digestion-method results are slightly lower than the optical results, but usually within their standard deviation.

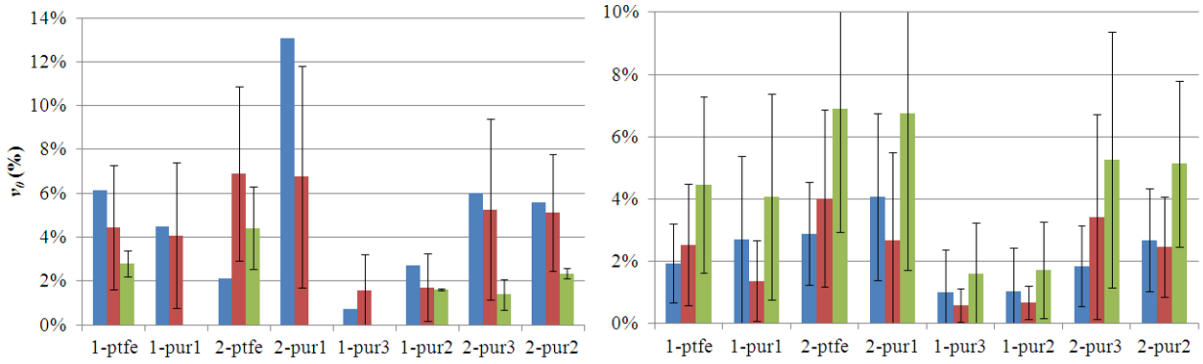

Figure 3. Left: average v_{0T} for volume comparison (blue), optical (red), and digestion (green) methods. Right: Average v_{0m} (blue), v_{0M} (red), and v_{0T} (green) by optical method.

The high standard deviation for the optical method (often ~100% of the mean) is partly due to the spatial variation. The digestion method was not applied to the "end" position for any laminate, resulting in less scatter. Figure 4 clarifies this by delineating v_0 by position. The samples by the end have the lowest v_0, as was the case with the infusions with DM in [10]. This could imply that flow under the membrane results in better VAP degassing, similar to the difference between natural and forced convection in heat transfer. This would also suggest that the void creation at the flow front by entrapment is outweighed by the pre-infusion air content in the resin. The difference between methods could be at least partially due to a significant difference in local v_{0T} despite the proximity of the optical and digestion samples.

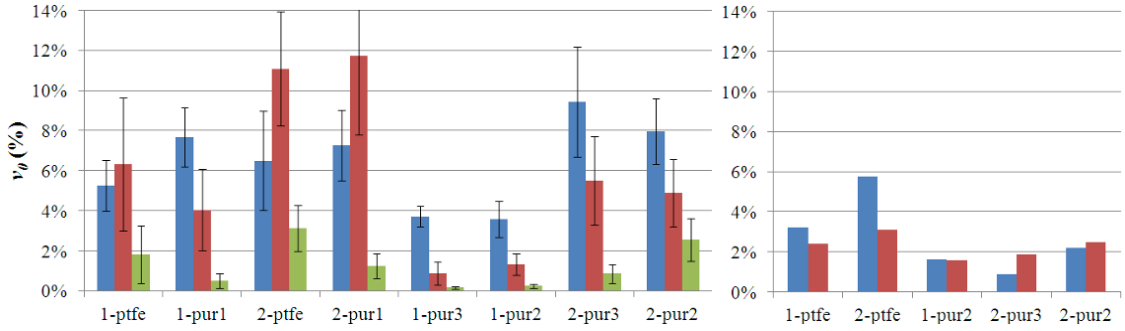

Figure 4. Average v_{0T} by optical method (left) and digestion method (right): inlet (blue), middle (red), end (green).

Figure 5 shows v_{0m} and v_{0M} by location for the optical method. Both v_{0m} and v_{0M} are once again lowest by the end. The difference in size and location of voids may be explained by the influence of dual scale flow. The resin flows faster in the inter-tow gaps at high pressures, but flows faster inside the tows due to capillary draw at low pressures. Bubbles are entrapped in the tows with the former, and in the inter-two gaps with the latter [9]. As the flow is fastest by the inlet, v_{0m} should be higher by the inlet, and v_{0M} should be higher by the end. Despite degassing, bubble movement and dissolution, this is generally the case. Samples by the inlet generally have the highest v_{0m}. Most of the samples from the middle have the highest v_{0M}.

Two interesting notes are that DM coverage of both sides actually resulted in higher v_0 for all cases, and the PTFE membranes resulted in no significant improvement over the PUR membranes. These are both contrary to results in [10], where v_0 decreased with the number of

DM-covered sides, and PTFE showed lower v_0. But the average v_0 in that study was very low (maximum 1.5%), signifying little difference between the infusions. The higher v_0 results in this study are thought to either be due to the resin choice (LY5052 seems to be more prone to voids) or less vacuum suction (50 mbar instead of 15 mbar as in [10]). In many RI type infusions using DM, the concentration of bubbles is high in the DM and lower in the laminate. The higher v_0 due to using double DM may be from increased air entrapment by using more DM. The location of the added layer (below the laminate) means that the entrapped bubbles may be pulled through the laminate's thickness towards the membrane, thus causing a higher v_0 inside the laminate. The rise in v_0 is most pronounced for the middle location. The v_0 measurements seem to be grouped in pairs in the order listed in the Figures. Each of the infusions was grouped in pairs and infused from the same resin pot. The order of pairs is the same order as listed in the v_0 graphs. An equal number of stirs were applied to each pot in an attempt to induce the same amount of porosity. But the pouring of the resin and hardener, which is more difficult to repeat, may be a significant factor in the v_0 of the resin pot. Thus, there is a chance that the resin pot's v_0 may affect the laminate v_0, e.g. the cause of the low v_0 for 1-pur3 and 1-pur2.

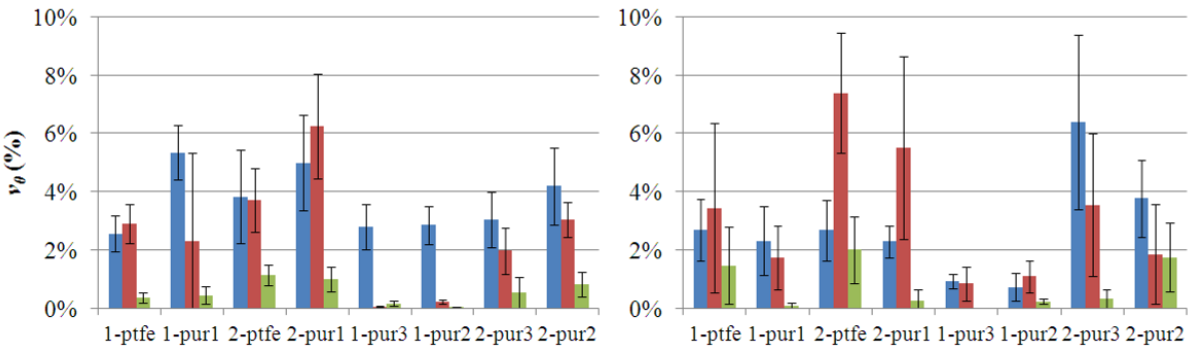

Figure 5. Average v_{0m} (left) and v_{0M} (right) by optical method: inlet (blue), middle (red), end (green).

3.4 Ultrasound c-scan correlation

The local c-scan ultrasound attenuation was measured for each sample tested for v_0. An example surface scan is shown in Figure 6. The ultrasonic absorption coefficient α (dB/mm) is the attenuation divided by the sample h as measured by microscopy. Figure 7 presents the correlation between α and v_0 by both optical and digestion methods. A similar linear increase in α with v_0 is seen, as has been reported elsewhere [5]. Thus, an estimate of the local porosity can be obtained by c-scan without having to do other methods of v_0 measurement.

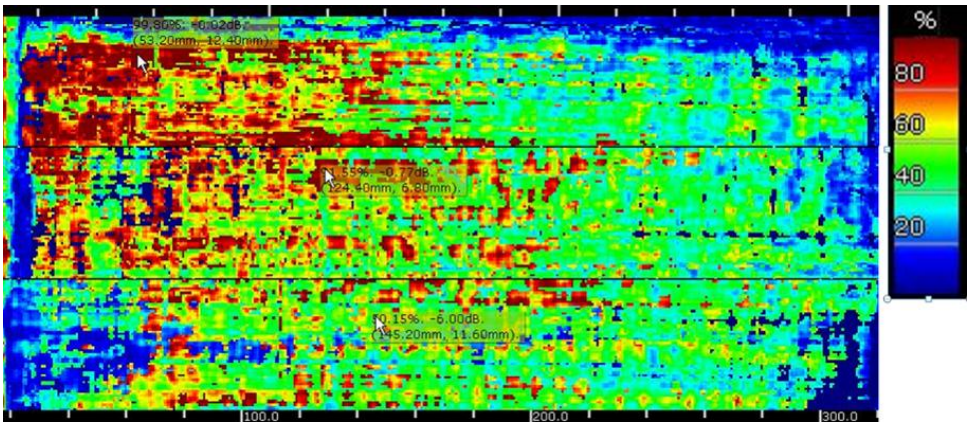

Figure 6. Sample c-scan of laminate surface showing percent signal attenuation.

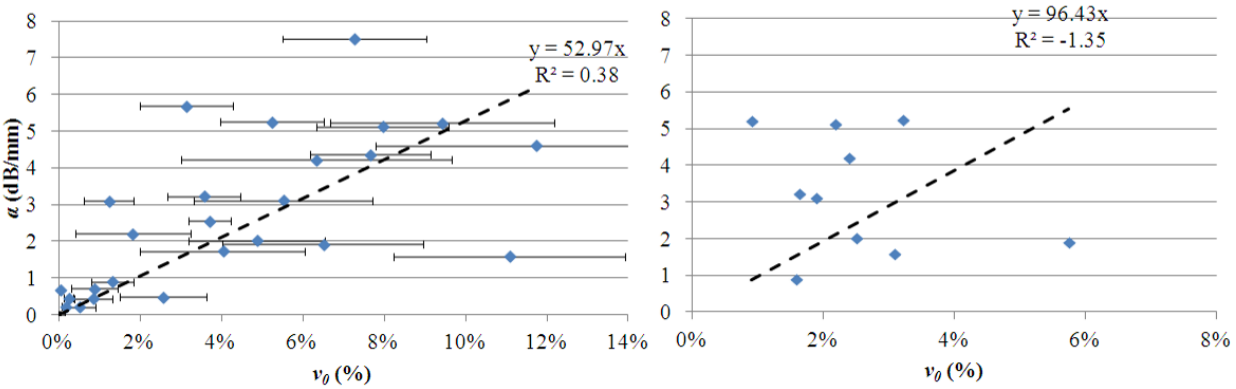

Figure 7. Ultrasound c-scan attenuation vs. v_0 (left = optical method, right = digestion method).

3.5 ILSS correlation

Shear properties for high-performance composite parts are important as they are a common mode of failure. The inter-laminar shear strength (ILSS) has shown to be highly sensitive to v_0, therefore many authors have focused on this property to characterize the effects of voids [5]. The average ILSS, τ, of all samples for each laminate was calculated, as well as the average for each of the three locations in optical v_0 measurement (by grouping samples close to the optical samples). Figure 8 shows the correlation between τ and v_{0T} by the three measurement methods, as well as the correlation against optical v_{0T} measurements when divided by position. All results imply a decrease of 1 to 2% in τ with each 1% increase in v_0. The results in [10] showed ~40% higher τ for v_{0T} = 0 implying better mechanical properties for that resin. A much steeper drop in τ was seen in [10]. As the range in v_0 was lower in that study, this may be due to initially steeper plots. A threshold v_0, beyond which little further change in mechanical properties occurs, has been suggested [4]. The linear fit is steeper when examining the same correlations grouped by v_{0m} and v_{0M} (Figure 9).

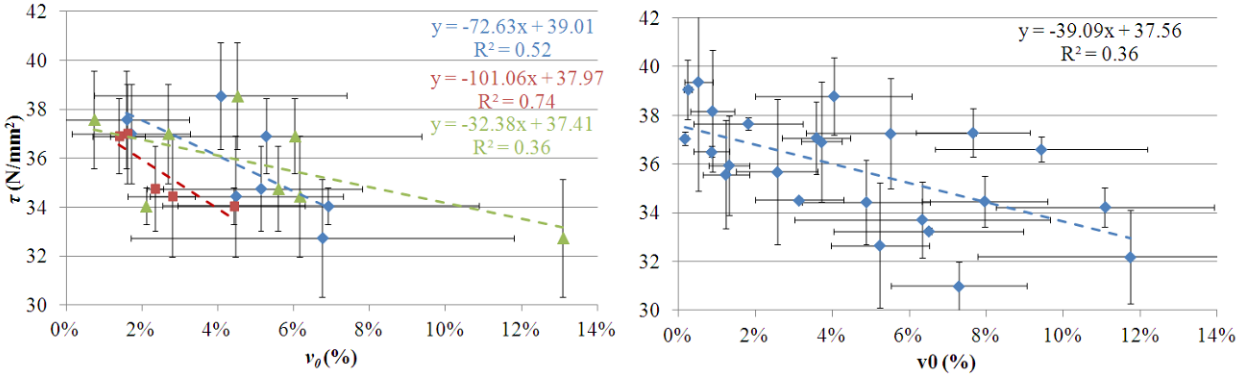

Figure 8. All laminates: v_{0T} vs. τ averaged for all positions (left) (♦ = optical, ■ = digestion, ▲ = mass), and for each position (right) (by optical method only).

Conclusions

The v_0 was lowest farthest from the inlet, suggesting that flow under the membrane may assist in VAP degassing. The greatest determinant of v_0 was how many sides were covered with DM, followed by the membrane choice, but pre-infusion resin bubbles may contribute to the differences. Only the PTFE membranes function with 120°C curing epoxies. The PTFE membranes degas as well or only slightly worse than PUR membranes for room temperature to 40°C processing. C-scan measurements proved that an estimate of the local void content

can be had from NDT methods. ILSS measurements confirmed a direct relationship between a low void content and high shear properties.

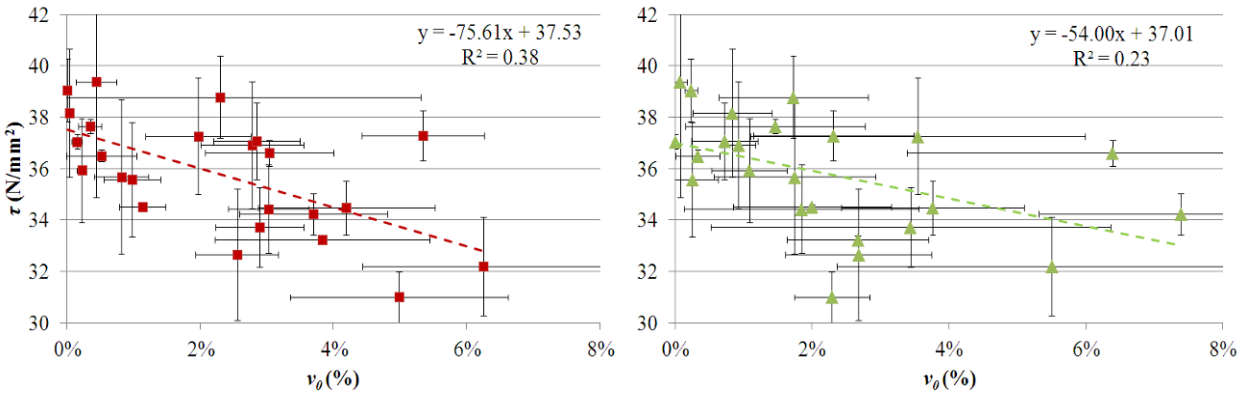

Figure 9. All laminates: v_0 vs. τ for each position, (left = micro voids, right = macro voids).

Acknowledgements

This study was partially funded by ReFACT, part of the Fifth Swedish National Aeronautical Research Program (NFFP5).

References

[1] Filsinger J., Lorenz T., Stadler F., Utecht S. *Method and device for producing fiber-reinforced components using an injection method.* U.S. Pat. 6,843,953, March 5, 2002.

[2] Li W., et al. Process and Performance Evaluation of the Vacuum-Assisted Process. *Journal of Composite Materials*, **38**, pp. 1803-1814 (2004).

[3] Cann M.T., Adams D.O., Schneider C.L. Characterization of fiber volume fraction gradients in composite laminates. *Journal of Composite Materials*, **42**, pp. 447-466 (2008).

[4] Liu L., Zhang B., Wang D., Wu Z. Effects of cure cycles on void content and mechanical properties of composite laminates. *Composite Structures*, **73**, pp. 303–309 (2006).

[5] Guo Z., Liu L., Zhang B., Du S. Critical Void Content for Thermoset Composite Laminates. *Journal of Composite Materials*, **43**, pp. 1775-1790 (2009).

[6] Gourichon B., Binetruy C., Krawczak P. A new numerical procedure to predict dynamic void content in liquid composite molding. *Composites: Part A*, **37**, pp. 1961–1969 (2006).

[7] Lundström T.S., Frishfelds V., Jakovics A. Bubble formation and motion in non-crimp fabrics with perturbed bundle geometry. *Composites: Part A*, **41**, pp. 83-92 (2010).

[8] Lundström T.S. Measurement of Void Collapse during Resin Transfer Moulding. *Composites: Part A*, **28A**, pp. 201-214 (1997).

[9] Leclerc J.S., Ruiz E. Porosity reduction using optimized flow velocity in Resin Transfer Molding. *Composites: Part A*, **39**, pp. 1859-1868 (2008).

[10] George A. *Optimization of Resin Infusion Processing for Composite Materials*. PhD thesis, University of Stuttgart (2011).